



Perpendicular magnetic anisotropy of Mn₄N films on MgO(001) and SrTiO₃(001) substrates

著者	Yasutomi Yoko, Ito Keita, Sanai Tatsunori, Toko Kaoru, Suemasu Takashi
journal or publication title	Journal of applied physics
volume	115
number	17
page range	17A935
year	2014-05
権利	(C) 2014 AIP Publishing LLC This article may be downloaded for personal use only. Any other use requires prior permission of the author and the American Institute of Physics. The following article appeared in J. Appl. Phys. 115, 17A935 (2014) and may be found at http://dx.doi.org/10.1063/1.4867955 .
URL	http://hdl.handle.net/2241/00121613

doi: 10.1063/1.4867955

Perpendicular magnetic anisotropy of Mn₄N films on MgO(001) and SrTiO₃(001) substrates

Yoko Yasutomi, Keita Ito, Tatsunori Sanai, Kaoru Toko, and Takashi Suemasu

Citation: *Journal of Applied Physics* **115**, 17A935 (2014); doi: 10.1063/1.4867955

View online: <http://dx.doi.org/10.1063/1.4867955>

View Table of Contents: <http://scitation.aip.org/content/aip/journal/jap/115/17?ver=pdfcov>

Published by the [AIP Publishing](#)

Articles you may be interested in

Magnetic properties of Mn₃O₄ film under compressive stress grown on MgAl₂O₄ (001) by molecular beam epitaxy

J. Appl. Phys. **114**, 053907 (2013); 10.1063/1.4817283

X-ray magnetic circular dichroism of ferromagnetic Co₄N epitaxial films on SrTiO₃(001) substrates grown by molecular beam epitaxy

Appl. Phys. Lett. **99**, 252501 (2011); 10.1063/1.3670353

Perpendicular magnetic anisotropy in CoFe₂O₄(001) films epitaxially grown on MgO(001)

J. Appl. Phys. **109**, 07C122 (2011); 10.1063/1.3566079

Structural and magnetic properties of La_{0.7}Sr_{0.3}MnO₃ thin films integrated onto Si(100) substrates with SrTiO₃ as buffer layer

J. Appl. Phys. **109**, 07C120 (2011); 10.1063/1.3565422

Structural and magnetic characterizations of Mn₂CrO₄ and MnCr₂O₄ films on MgO(001) and SrTiO₃(001) substrates by molecular beam epitaxy

J. Appl. Phys. **109**, 07D714 (2011); 10.1063/1.3545802



AIP | Journal of Applied Physics

Journal of Applied Physics is pleased to announce **André Anders** as its new Editor-in-Chief

Perpendicular magnetic anisotropy of Mn₄N films on MgO(001) and SrTiO₃(001) substrates

Yoko Yasutomi, Keita Ito, Tatsunori Sanai, Kaoru Toko, and Takashi Suemasu^{a)}

Institute of Applied Physics, Graduate School of Pure and Applied Sciences, University of Tsukuba, 1-1-1 Tennodai, Tsukuba, Ibaraki 305-8573, Japan

(Presented 8 November 2013; received 23 September 2013; accepted 6 December 2013; published online 11 March 2014)

We grew Mn₄N epitaxial thin films capped with Au layers on MgO(001) and SrTiO₃(001) substrates by molecular beam epitaxy. Perpendicular magnetic anisotropy (PMA) was confirmed in all the samples at room temperature from the magnetization versus magnetic field curves using superconducting quantum interference device magnetometer. From the ω -2 θ x-ray diffraction (XRD) and ϕ -2 θ_χ XRD patterns, the ratios of perpendicular lattice constant c to in-plane lattice constant a , c/a , were found to be about 0.99 for all the samples. These results imply that PMA is attributed to the in-plane tensile strain in the Mn₄N films. © 2014 AIP Publishing LLC. [<http://dx.doi.org/10.1063/1.4867955>]

In recent years, new functional spintronics devices such as spin-transfer torque random access memory¹ and current-driven domain wall motion nonvolatile memory² have been proposed. In such devices, materials that give high spin polarization in electron transport need to be sought. Therefore, highly spin polarized materials have attracted much attention from both the theoretical and experimental points of view.^{3–6} We have done a lot of research on inverse perovskite ferromagnetic nitride (Co,Fe)₄N. This material is theoretically predicted to have negative but large spin polarization.^{7–9} So far, we succeeded in epitaxial growth of Fe₄N, Co₄N, and (Co,Fe)₄N thin films on SrTiO₃(STO)(001) substrates by molecular beam epitaxy (MBE),^{10–12} and evaluated the spin and orbital magnetic moments per Co and Fe atoms by x-ray magnetic circular dichroism,^{13,14} and other basic properties such as spin-resolved valence band structure and negative anisotropic magneto resistance effect.^{15,16} Among ferromagnetic nitrides, there have been a very limited number of reports about perpendicular magnetic anisotropy (PMA) in Mn₄N films thus far.^{17–20} PMA has attracted increasing interest, because it is useful for spintronics devices like low current-induced magnetization switching magnetic tunnel junction devices²¹ and others. A lot of studies have been done on Co₂FeAl,²² CoFeB,²³ and CoFe₂O₄ films.^{24,25} PMA is considered to be caused by the magnetoelastic coupling due to the in-plane tensile strain in the CoFe₂O₄ thin films.^{24,25} PMA was observed in the Mn₄N films on Si(001) by reactive sputtering,^{17,18} and those on SiC(0001) by MBE.²⁰ However, they did not measure the lattice constants in the films. Thus, the origin of PMA was not fully understood. Recently, Tsunoda and Kabara prepared a 50-nm-thick Mn₄N film on MgO by reactive sputtering.¹⁹ They attributed the observed PMA to the in-plane tensile strain because the ratio of perpendicular lattice constant c to in-plane lattice constant a , c/a , was found to be approximately 0.99. In this work, we attempted to grow Mn₄N thin films epitaxially on MgO(001) and STO(001) substrates by MBE, and investigated the influence of lattice mismatch on the magnitude of in-plane strain

and PMA in the films. The lattice mismatches for Mn₄N(001)/MgO(001) and Mn₄N(001)/STO(001) are -8% and -1% , respectively.

We grew Mn₄N thin films on MgO(001) and STO(001) substrates using a solid source Mn and radio-frequency N₂ plasma at a substrate temperature of 450 °C.²⁶ After the growth, the films were *in-situ* covered with Au at room temperature (RT) in the same MBE chamber to prevent oxidation of the surfaces. Samples were prepared as summarized in Table I. The crystal quality of grown layers was evaluated by reflection high-energy electron diffraction (RHEED), ω -2 θ Cu- K_α x-ray diffraction (XRD) and ϕ -2 θ_χ XRD. Ge(220) single crystals were used to make x-rays monochromatic. Au/Mn₄N layer thicknesses were evaluated using a conventional surface profiler. The magnetization versus magnetic field (M - H) curve was measured at RT using the superconducting quantum interference device (SQUID) magnetometer. The external magnetic field (H) of -5 – 5 T was applied in the normal and in-plane directions of samples.

Streaky RHEED patterns were obtained for all the samples. Figures 1(a)–1(d) show the out-of-plane ω -2 θ XRD patterns of samples A–D, respectively. The diffraction peaks of Mn₄N(002) and (004) were observed in all the samples. Figures 2(a)–2(d) show the in-plane ϕ -2 θ_χ XRD patterns of samples A–D, respectively. The scattering vector was set along the MgO[100] and STO[100] directions. Similarly, the diffraction peaks of Mn₄N(200) and (400) were observed in all the samples. These results mean that the Mn₄N thin films were epitaxially grown on MgO(001) and STO(001) substrates. From the results of XRD measurements, we calculated the c/a ratios in samples A–D as summarized in Table I. The c values were 0.386, 0.387, 0.387, and 0.386 nm in samples A–D, and the a values were 0.390, 0.391, 0.389, and 0.390 nm, in samples A–D, respectively. Therefore, the c/a ratios were calculated to be 0.991, 0.990, 0.995, and 0.989, respectively. These results show that the in-plane tensile strain existed in all the Mn₄N films. It is very important to notice here that the c/a ratios were almost the same in samples A–D, in spite of the different substrates and different Mn₄N layer thicknesses. Thus, we speculate that the in-plane tensile strain was not caused by the lattice

^{a)}Author to whom correspondence should be addressed. Electronic mail: suemasu@bk.tsukuba.ac.jp.

TABLE I. Sample preparation: substrate, Mn_4N layer thicknesses, Au layer thickness, and c/a ratios are shown.

Sample	Substrate	Mn_4N (nm)	Au (nm)	c/a ratio
A	MgO(001)	12	4	0.991
B	STO(001)	12	4	0.990
C	MgO(001)	26	5	0.995
D	STO(001)	28	5	0.989

mismatch but by other factors, for example, difference in thermal expansion coefficient between substrate and Mn_4N . The c/a ratio of 0.99 was also observed even in the 50-nm-thick Mn_4N film.¹⁹ Another possibility is that 12 nm in sample A was already too thick to make the Mn_4N films pseudomorphic.

Figures 3(a)–3(d) show the M - H curves of samples A–D, respectively, measured by SQUID magnetometer at RT. We deduced the diamagnetic component of the substrates from the slope of raw M - H curves at large H region, and subtracted it from the raw data. The magnetization of the films was saturated at such large H regions. We see that the hysteresis curves were clearly open in all the samples when H was applied perpendicular to the films. On the other hand, the hysteresis curves were closed when H was applied in the in-plane direction. These results show that PMA surely appeared in the Mn_4N films. The saturation magnetization (M_S) value was approximately 145 emu/cc in samples A–D. This value is larger than that reported (110 emu/cc) in the Mn_4N film on MgO(001) at 300 K.¹⁹ The coercive field and anisotropic magnetic field (H_K) were approximately 2.5 k and 30 kOe, respectively. The total uniaxial magnetic anisotropy

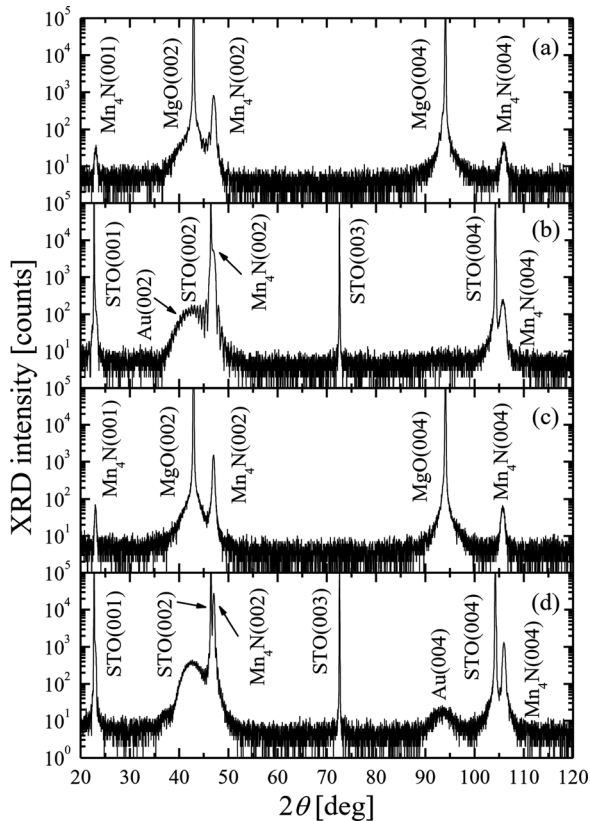


FIG. 1. Out-of-plane ω - 2θ XRD patterns for (a) sample A, (b) sample B, (c) sample C, and sample D.

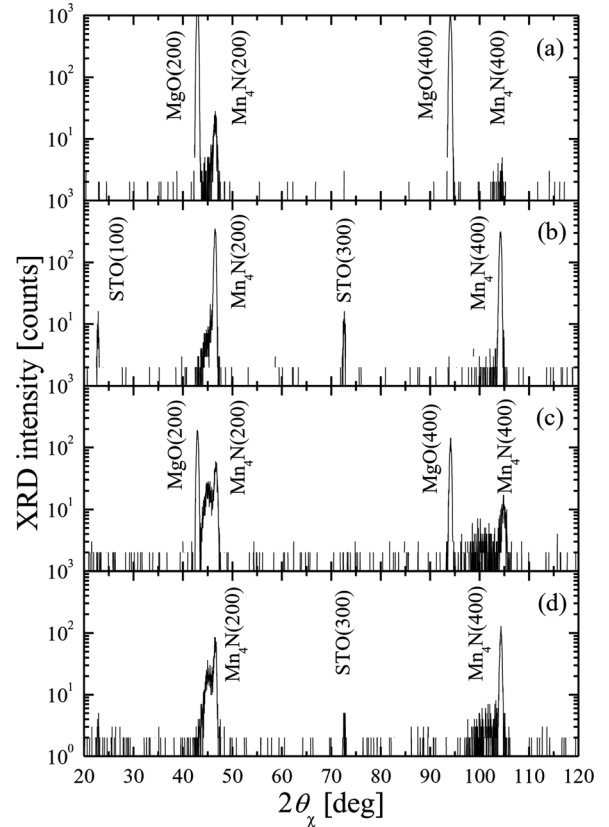


FIG. 2. In-plane ϕ - $2\theta_\chi$ XRD patterns of (a) sample A, (b) sample B, (c) sample C, and (d) sample D.

energy ($E_A = M_S H_K / 2$) was deduced to be approximately 2.2 Mergs/cc for samples A–D. This value is twice as large as that reported in the Mn_4N film on MgO(001) substrates by reactive sputtering ($E_A \sim 1.0$ Mergs/cc).¹⁹

E_A in the perpendicular magnetization film is given by (Refs. 22 and 23)

$$E_A = K^V + \frac{K^I}{t} - 2\pi M_S^2, \quad (1)$$

where K^V is the volume anisotropy energy, K^I the interfacial anisotropy energy, t the ferromagnetic film thickness, and $-2\pi M_S^2$ the shape anisotropy energy. As for the presence of the interfacial PMA, there have been no reports in $\text{Mn}_4\text{N}/\text{MgO}$ and $\text{Mn}_4\text{N}/\text{STO}$. We think that the contribution of K^I/t term to PMA is small, if any, because the Mn_4N layer thickness t was thicker than 12 nm in samples A–D. In the case of $\text{Co}_2\text{FeAl}/\text{MgO}$ and CoFeB/MgO , interfacial PMA was confirmed only in very thin films (~ 1 nm).^{22,23} On the other hand, PMA was observed even in much thicker Mn_4N films (50 nm).¹⁹ This means that PMA was observed even when the K^I/t term was small in the Mn_4N film, implying that the interfacial energy plays a minor role in the appearance of PMA. Thus, we suppose that PMA was induced in the Mn_4N films, that is $E_A > 0$, because of $K^V > 2\pi M_S^2$. When the c -axis-oriented cubic thin film receives tensile strain in the in-plane direction, it becomes tetragonal. The uniaxial magnetic anisotropy energy induced by magnetoelastic coupling (K_U^V) is given by (Ref. 24)

$$K_U^V = -\frac{3}{2} \lambda_{100} (C_{11} - C_{12}) \left(\frac{a-c}{a_0} \right), \quad (2)$$

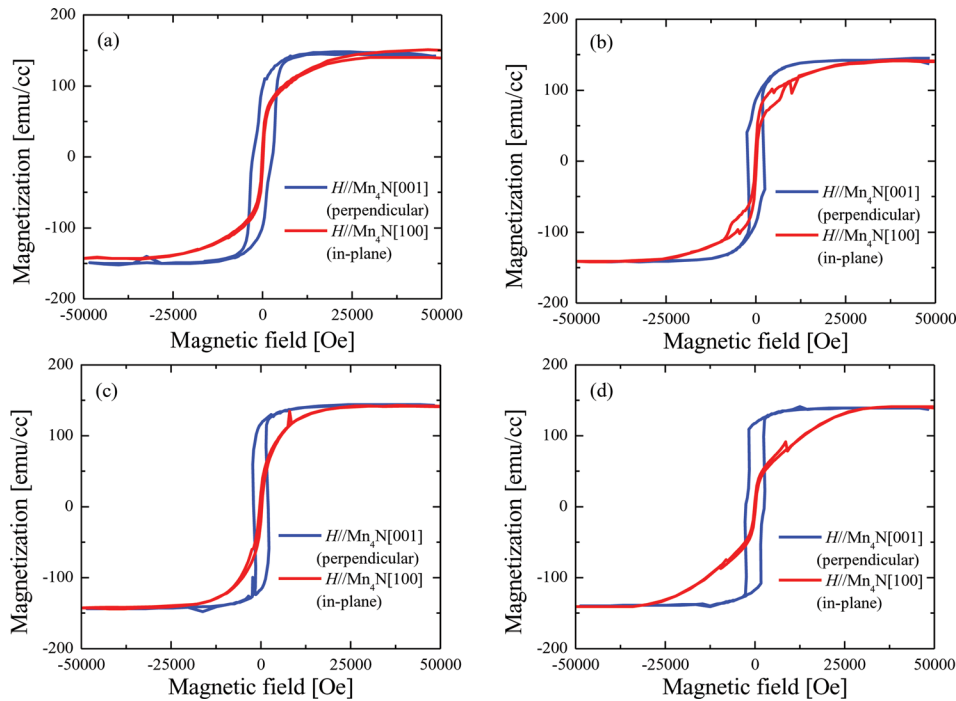


FIG. 3. M - H curves of (a) sample A, (b) sample B, (c) sample C, and (d) sample D, measured at RT. H was applied normal and parallel to the samples.

where λ_{100} is the magnetostriction constant along the [100] orientation of the magnetic thin film. C_{11} and C_{12} the elastic moduli in the directions perpendicular and parallel to the surface, respectively, a_0 the bulk lattice constant. λ_{100} is negative in Mn_4N .^{17,18} It is reasonable to think that C_{11} is greater than C_{12} in most of cubic metals and therefore in inverse perovskite nitrides.^{27,28} The presence of in-plane tensile strain ($c < a$) thus gives rise to $K_V^V > 0$ in samples A–D. We therefore conclude that positive K_V^V and small $2\pi M_S^2$ caused PMA in the Mn_4N films. This mechanism of PMA is similar to that in CoFe_2O_4 films.^{24,25} The value of $-2\pi M_S^2$ was -0.13 Mergs/cc in samples A–D, which means that the K_V^V value is 2.3 Mergs/cc because E_A is 2.2 Mergs/cc. About the magnetocrystalline anisotropy, the easy magnetization axis of bulk Mn_4N is along the $\langle 111 \rangle$ axes.²⁹ However, there have been no reports on the magnetocrystalline anisotropy energy in both cubic and pseudomorphic Mn_4N . We measured the in-plane M - H curves along the [100] and [110] axes of Mn_4N films on STO. However, significant difference was not observed in the hysteresis curves. This means that contribution of magnetocrystalline anisotropy to the PMA can be considered to be small. Similar discussions were made in Ref. 30. Magnetic torque measurements help us distinguish the contribution of magnetocrystalline anisotropy from the others in Mn_4N films.³¹ It is true that dependence of PMA on c/a ratio enables us to clarify the origin of PMA much more strongly. But the fact that all the Mn_4N films with $c/a < 1$ showed clear PMA implies that the observed PMA was caused by the in-plane tensile stress in the Mn_4N .

In summary, we grew Mn_4N epitaxial thin films of different layer thicknesses on two kinds of substrates, $\text{MgO}(001)$ and $\text{STO}(001)$, by MBE. PMA was clearly observed in the M - H curves for all the samples at RT. The c/a ratios in the Mn_4N films were found to be approximately 0.99 from the XRD measurements for all the samples regardless of the different substrates and the different layer

thicknesses. We therefore attributed the observed PMA to the in-plane tensile strain in the Mn_4N films.

The authors thank Dr. M. Tsunoda of Tohoku University for useful discussion. M - H curves measurements were performed with the cooperation of Dr. R. Akiyama, Dr. K. Suzuki, Dr. H. Yanagihara, Dr. T. Koyano, Professor S. Kuroda, and Professor E. Kita of University of Tsukuba.

¹K. Miura *et al.*, in *Proceedings of the International Symposium on VLSI Technology* (2007), p. 234.

²S. S. P. Parkin *et al.*, *Science* **320**, 190 (2008).

³S. Picozzi *et al.*, *Phys. Rev. B* **66**, 094421 (2002).

⁴Y. Sakuraba *et al.*, *Jpn. J. Appl. Phys., Part 2* **44**, L1100 (2005).

⁵Y. K. Takahashi *et al.*, *Appl. Phys. Lett.* **98**, 152501 (2011).

⁶A. Schmehl *et al.*, *Nature Mater.* **6**, 882 (2007).

⁷S. Kokado *et al.*, *Phys. Rev. B* **73**, 172410 (2006).

⁸Y. Imai *et al.*, *J. Magn. Magn. Mater.* **322**, 2665 (2010).

⁹Y. Takahashi *et al.*, *J. Magn. Magn. Mater.* **323**, 2941 (2011).

¹⁰K. Ito *et al.*, *J. Cryst. Growth* **322**, 63 (2011).

¹¹K. Ito *et al.*, *J. Cryst. Growth* **336**, 40 (2011).

¹²T. Sanai *et al.*, *J. Cryst. Growth* **357**, 53 (2012).

¹³K. Ito *et al.*, *Appl. Phys. Lett.* **98**, 102507 (2011).

¹⁴K. Ito *et al.*, *Appl. Phys. Lett.* **99**, 252501 (2011).

¹⁵K. Ito *et al.*, *J. Appl. Phys.* **112**, 013911 (2012).

¹⁶K. Ito *et al.*, *Jpn. J. Appl. Phys., Part 1* **51**, 068001 (2012).

¹⁷K. M. Ching *et al.*, *J. Appl. Phys.* **76**, 6582 (1994).

¹⁸K. Ching *et al.*, *Appl. Surf. Sci.* **92**, 471 (1996).

¹⁹M. Tsunoda and K. Kabara, in *International Conference of the Asian Union of Magnetism Societies (ICAUMS)* (2012), 2pPS-47.

²⁰S. Dhar *et al.*, *Appl. Phys. Lett.* **86**, 112504 (2005).

²¹T. Kishi *et al.*, *Tech. Dig. - Int. Electron Devices Meet.* **2008**, 309–312.

²²Z. Wen *et al.*, *Appl. Phys. Lett.* **98**, 242507 (2011).

²³S. Ikeda *et al.*, *Nature Mater.* **9**, 721 (2010).

²⁴A. Lisfi *et al.*, *Phys. Rev. B* **76**, 054405 (2007).

²⁵H. Yanagihara *et al.*, *J. Appl. Phys.* **109**, 07C122 (2011).

²⁶H. Yang *et al.*, *J. Appl. Phys.* **91**, 1053 (2002).

²⁷C. Kittel, *Introduction to Solid State Physics*, 8th ed. (Wiley, Hoboken, NJ, 2005), p. 84.

²⁸Z. Wu and J. Meng, *Appl. Phys. Lett.* **90**, 241901 (2007).

²⁹D. Fruchart *et al.*, *J. Phys. F: Met. Phys.* **9**, 2431 (1979).

³⁰P. C. Dorsey *et al.*, *J. Appl. Phys.* **79**, 6338 (1996).

³¹T. Niizeki *et al.*, *Appl. Phys. Lett.* **103**, 162407 (2013).